Avoiding the Polarization Catastrophe in $LaAlO_3$ Overlayers on $SrTiO_3(001)$ through Polar Distortion

Rossitza Pentcheva[1] and Warren E. Pickett[2]

[1]*Department of Earth and Environmental Sciences, University of Munich, Theresienstr. 41, 80333 Munich, Germany*
[2]*Department of Physics, University of California, Davis, One Shields Avenue, Davis, California 95616, USA*

A pronounced uniform polar distortion extending over several unit cells enables thin $LaAlO_3$ overlayers on $SrTiO_3(001)$ to counteract the charge dipole and thereby neutralize the "polarization catastrophe" that is suggested by simple ion counting. This unanticipated mechanism, obtained from density functional theory calculations, allows several unit cells of the $LaAlO_3$ overlayer to remain insulating (hence, fully ionic). The band gap of the system, defined by occupied O $2p$ states at the surface and unoccupied Ti $3d$ states at the interface in some cases $\sim$20 Å distant, decreases with increasing thickness of the $LaAlO_3$ film before an insulator-to-metal transition and a crossover to an electronic reconstruction occurs at around five monolayers of $LaAlO_3$.

Heterostructures containing polar [e.g., $LaAlO_3$ (LAO)] and nonpolar [e.g., $SrTiO_3$ (STO)] oxides raise issues similar to semiconductor heterostructures, e.g., Ge/GaAs [1]. If the ionic charges are maintained, then adding LAO layers (with alternating positively charged LaO and negatively charged AlO_2-layers) onto an STO substrate is expected to lead to an ever-increasing dipole. The accompanying potential shift across the LAO slab should eventually cause a "polarization catastrophe"[2,3]. To avoid this, surfaces are supposed to reconstruct (atomically, e.g., via defects) or facet [4]. However, in oxides containing transition metal ions, further compensation mechanisms are available. These can lead to electronic phenomena that are unanticipated from the properties of the bulk constituents and can thus invoke new functionality. Although LAO and STO are two conventional nonmagnetic band insulators, a high conductivity [5] as well as indications for magnetism [6] and superconductivity [7] were measured at the n-type LaO/TiO_2 interface (IF). The initially reported high carrier density was subsequently found to be sensitive to film growth conditions [2,6,8–12] and for annealed samples, the sheet resistance increases by several orders of magnitude [6].

Recently, a thickness dependent switching between insulating and conducting behavior [13] was reported around four monolayers (MLs) of LAO on STO(001). Thiel *et al.* [13] found that the insulator-to-metal transition can also be induced dynamically by an external electric field. Writing and erasing of nanoscale conducting regions in LAO overlayers on $SrTiO_3(001)$ was demonstrated [14] with an applied local electric field (by atomic force microscope). In contrast to the abrupt transition in LAO films on STO(001), Huijben and collaborators [15] observed a smoother increase in carrier density when the LAO film was covered by $SrTiO_3$. These results lend additional urgency to understand the insulator-to-metal switching in oxide nanostructures.

The seeming violation of charge neutrality has become a central consideration in trying to understand the unexpected behavior that emerges at the interface. So far, theoretical efforts have concentrated mainly on LAO/STO superlattices [16–23]. For these, density functional theory calculations (DFT) suggest that the charge mismatch at the electron doped n-type interface is accommodated by partial occupation of the Ti $3d$ band. Within $LDA(GGA) + U$ [24], the excess charge is localized in the interface layer with a checkerboard arrangement of Ti^{3+} and Ti^{4+} [16,22,23].

At first glance, the transition from insulating to conducting behavior found between three and four LAO ML on $SrTiO_3(001)$ [13] does not fit into the picture obtained from the $GGA + U$ calculations for infinitely extended superlattices [16,23]. In the latter, the charge mismatch is accommodated immediately at the IF and largely independent of the thickness of LAO and STO.

Here, we shed light on the nature of the electronic state at the interface and the origin of thickness dependent metal-to-insulator transition. Based on DFT-calculations, we demonstrate that an interface between a thin LAO film on a STO(001) substrate is fundamentally different from an IF in a periodic superlattice. In a thin overlayer, there are two polar discontinuities, one at the IF and another at the surface. As we will show in this Letter, the proximity to the surface and the associated atomic relaxation has a profound effect on the properties and compensation mechanism at the interface.

To address these issues, we study here the structural and electronic properties of 1–5 ML of LAO on a STO(001)-substrate, and contrast them to the behavior of LAO/STO superlattices. The DFT calculations are performed with the all-electron full-potential augmented plane waves (FP-APW) method in the WIEN2K-implementation [25] and generalized gradient approximation (GGA) [26] of the exchange-correlation potential. We have used the lateral
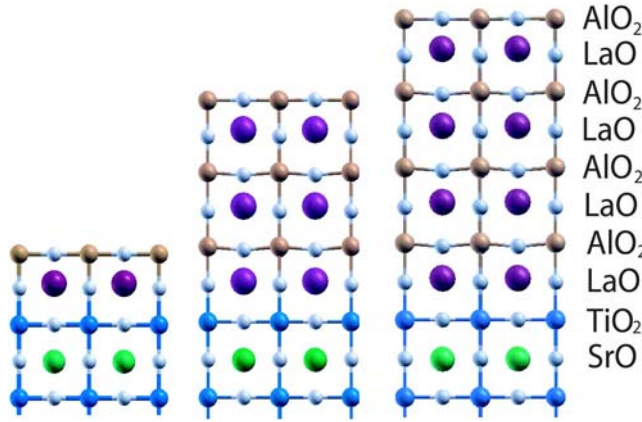
FIG. 1 (color online). Side view of the relaxed structures of 1, 3, and 4 ML LAO on STO(001) showing the polar distortion. The oxygen ions are marked by light grey spheres, while the Sr-, La-, Ti-, and Al-cations are shown by large green (grey), purple (dark grey) and small blue (dark grey) and orange (grey) spheres.

FIG. 2 (color online). Vertical displacements of ions Δz in the (a) AO and (b) BO_2 layers with respect to the bulk positions in Å for 1–5 MLs of LAO on STO(001) obtained within GGA. Cation/oxygen relaxations are marked by full black/open red (grey) symbols. The corresponding layer-resolved dipole moments are displayed in (c). The x axis shows the distance from the interface (I) TiO_2-layer.

lattice constant of the $SrTiO_3$-substrate obtained from GGA (3.92 Å) because it is in closer agreement with the experimental value (3.905 Å) [27]. Thus, the epitaxial $LaAlO_3$-film (3.79 Å) is subject to tensile strain on $SrTiO_3$ due to a lattice mismatch of 3%. The GGA-gap for bulk $SrTiO_3$ is 2.0 eV ($\Delta^{\text{expt}} = 3.2$ eV) separating filled O $2p$ bands and unfilled Ti $3d$ bands. For $LaAlO_3$, we obtain a band gap within GGA of 3.7 eV ($\Delta^{\text{expt}} = 5.6$ eV) between filled O $2p$ bands hybridized with Al p-bands and unfilled conduction bands comprised of La $5d$ and Al $3s$, $3p$ states.

The thin (1–5 ML) LAO films on a STO(001) substrate were modeled in the supercell geometry with two inversion symmetric surfaces to avoid spurious electric fields. We have ensured convergence with respect to the substrate thickness: Calculations for 3 ML LAO/STO(001) using two and six monolayers of STO substrate rendered the same structural and electronic behavior of the system. To minimize the interaction between neighboring surfaces, the slabs are separated in the z-direction by 10–12 Å of vacuum. Because surface x-ray (SXRD) [28] and low energy electron diffraction [29] measurements give no indication for a superstructure, we have considered only defect-free unreconstructed surfaces.

Polar distortions.—A full structural optimization was performed within the tetragonal unit cell using GGA. The relaxed structures are pictured in Fig. 1, and the atomic displacements which are exclusively along the c-axis are plotted in Fig. 2.

An unexpected pattern is uncovered: (i) The surface AlO_2 layer shows an inward relaxation of both Al (0.12–0.19 Å) and O (0.11–0.15 Å) atoms by similar amounts, resulting in only a small buckling of 0.01–0.04 Å. (ii) The most striking result is a strong buckling in all LaO layers with a uniform polar-type distortion of 0.20–0.36 Å. This relaxation is dominated by the outward movement of La by
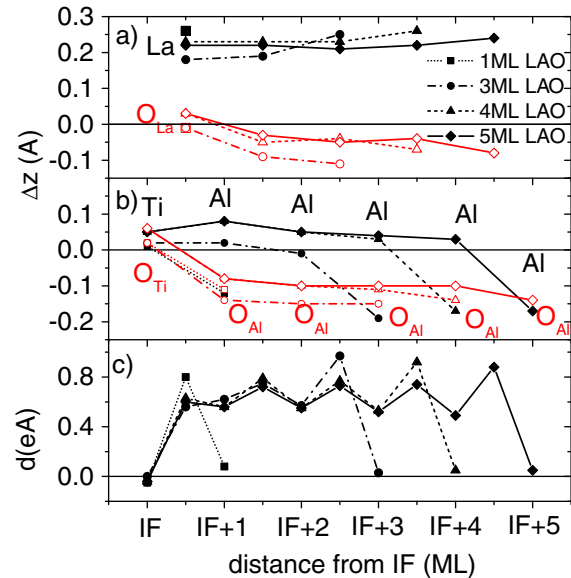
up to 0.26 Å. (iii) The subsurface AlO_2 layers are also buckled by approx. 0.15 Å: Al relaxes outward by 0.01–0.08 Å, O inward by $\sim$0.10 Å. (iv) The Ti and O-ions at the interface show only small outward relaxation (less than 0.06 Å). This situation of large polar distortions throughout the LAO slab with negligible distortion in STO contrasts strongly the behavior obtained for $LaAlO_3$ (or $LaTiO_3$)/$SrTiO_3$ superlattices where ferroelectric-like plane buckling is predominantly in the TiO_2 layer at the interface [17–20,30,31] and amounted to 0.17 Å for a 5LAO/5STO heterostructure [23].

Although not explicitly discussed, previous VASP calculations showed a similar relaxation pattern [14]. In contrast, another WIEN2K study reported only small relaxations [32] also finding metallic behavior for all LAO thicknesses. Vonk *et al.* [28] performed an SXRD analysis for a LAO overlayer on STO(001) with a total thickness of 0.5 MLs. The best fit infers a contracted TiO_6 octahedron at the interface and an outward relaxation of La in the LaO layer. A direct comparison to our results is not possible because of the different coverage and since the incomplete LAO layer allows for lateral relaxations of strain.

Compensating electronic and ionic dipoles.—The implied dipole moment of a 4 ML $LaAlO_3$ film is $\mathcal{D}_{\text{bare}} \approx -0.5e \times (3.9 \text{ Å}) \times 4 \text{ cells} = -7.8e$ Å which translates into a bare potential shift across the four LAO-layer slab of 80–90 eV. This electric field is screened by electronic *plus* ionic polarization. Using the bulk LAO dielectric constant
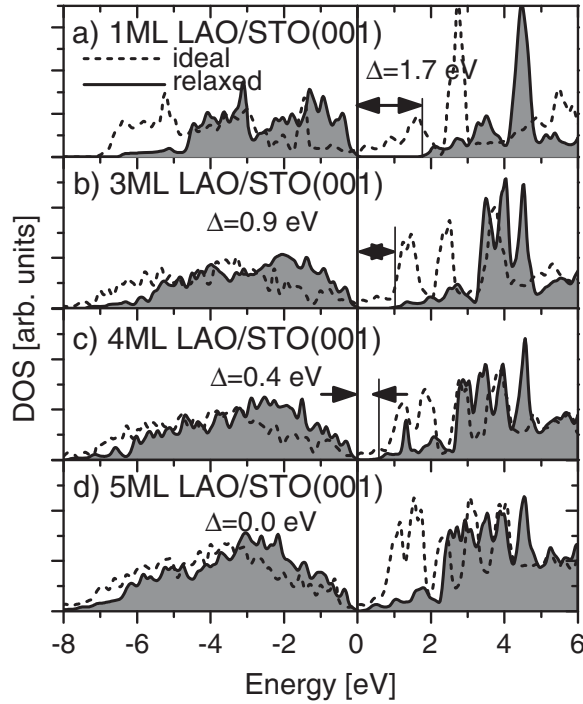
FIG. 3.   Density of states for the ideal (dashed line) and relaxed (solid line, grey filling) structure of 1–5 ML LAO on STO(001). Relaxation opens a band gap, but its size decreases with each added LAO layer.

$\epsilon = 24$, this becomes approximately $\Delta V = 4\pi e \frac{\mathcal{D}_{bare}}{\epsilon (3.9 \text{ Å})^2} \sim$ 3.5 eV, which can be sustained by the 5.6 eV gap of LAO.

The dipole shift due to the polar distortion can be estimated from the displacements, using for simplicity the formal ionic charges [33]. The layer-resolved dipoles, pictured in Fig. 2, show a strikingly uniform behavior in the inner LAO layers (a strong dipole moment of ~ 0.55 and $\sim 0.75 e$ Å in the AlO$_2$ and LaO layers, respectively) and an almost vanishing dipole in the interface TiO$_2$ and surface AlO$_2$ layers. The total ionic dipole, e.g., for the 4 ML LAO film is

$$\mathcal{D} = \sum_i Z_i \Delta z_i \approx 4.8 e \text{ Å}. \qquad (1)$$

This rough estimate gives a value that is more than 60% of $\mathcal{D}_{bare}$ and of opposite sign. The large polar distortion has a significant impact on the electronic behavior of the system (LAO film + STO substrate).

Electronic properties of overlayer + interface.—The total density of states as a function of the LAO thickness for 1–5 ML thick LAO films on STO(001) is shown in Fig. 3. For the ideal atomic positions, all systems are metallic due to an overlap of the surface O $2p$ bands with the Ti $3d$ bands at the interface (cf. Fig. 4). The strong lattice polarization leads to insulating behavior for $N = 1$–4 ML. With increasing thickness of the LAO-film, the gap decreases by approximately 0.4 eV per added LAO layer starting from
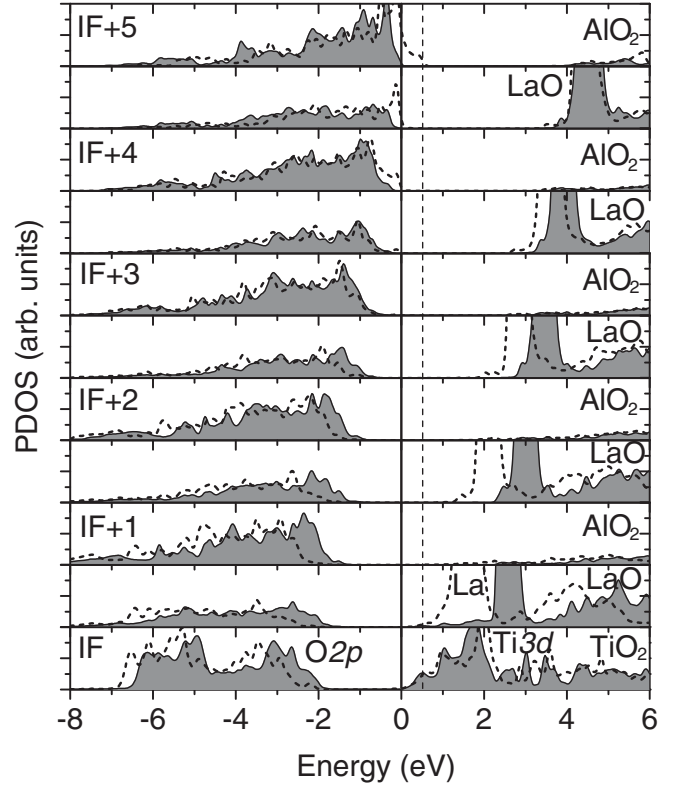

FIG. 4.   Layer-resolved density of states of 5 ML LAO on STO (001) with ideal (dashed line) and relaxed (grey shaded area) coordinates. The DOS for the ideal positions was shifted by 0.5 eV to align with the conduction band of the system with the relaxed atomic positions. Its Fermi level is marked with a dashed line.

1.7 eV for 1 ML LAO and finally closes for 5 ML LAO/ STO(001). While the DFT calculations correctly predict an insulator-to-metal transition, the critical thickness θ_{crit} is affected by the band gap underestimation within GGA and is expected to occur beyond an LAO thickness of 6 MLs for a defect-free surface. Defects and/or adsorbates which are not considered in the theoretical model may be responsible for the lower θ_{crit} found in experiment [13].

In order to gain more insight into the type of electronic states around the Fermi level and their spatial distribution, we have plotted in Fig. 4 the layer-resolved density of states for 5 ML LAO/STO(001) with ideal and relaxed atomic positions. A nearly rigid upward shift of the O $2p$-bands towards the Fermi level is observed as they approach the surface. For the relaxed configuration, the top of the valence band is determined by the O $2p$ band in the surface AlO$_2$ layer, while the bottom of the conduction band is fixed by the unoccupied Ti $3d$ band at the interface. Thus, the closing of the gap is due to the raising of the O $2p$ valence band states in the surface LAO layer as the LAO slab gets thicker.

For an isolated *n*-type IF (in LAO/STO superlattices), the "extra" $0.5 e^-$ per IF Ti ion cannot go into the LAO

layers due to the large band gap, and it remains at the IF and charge-orders (within GGA + U) rather than occupy itinerant Ti $3d$ states within the STO layers [16,23]. In contrast, in thin LAO overlayers, the lattice screening reduces the net electric field and thus allows the system to preserve the formal ionic charges. Since these correspond to closed shells, including correlation effects within LDA + U would have only a minor influence on the result [34]. Thus, up to 5ML, there is no need for an electronic (or atomic) reconstruction. However, beyond θ_{crit}, the ionic screening mechanism breaks down and a small concentration of charge carriers emerges: holes at the surface and electrons at the interface. This results in a weak conductivity, consistent with hard x-ray photoemission measurements [12] and recent theoretical results [35].

In summary, strong lattice polarization compensates the dipolar electric field in thin LAO overlayers and sustains the insulating behavior up to 5 MLs LAO. The effect of this polar distortion is crucial: Without it, the system is metallic for any coverage of LaAlO$_3$. The band gap in the relaxed systems formed between two spatially separated bands—O $2p$ states in the surface layer and Ti $3d$ states at the interface—decreases gradually and collapses at 5 ML LAO/STO(001) giving rise to an electronic reconstruction as the system approaches the limit of the isolated interface.

The structural distortion we observe here differs from issues discussed for ultrathin ferroelectric films, e.g., the existence of a critical thickness below which ferroelectric displacements are suppressed [36–39]. In contrast, LaAlO$_3$ is a wide band gap insulator with a low dielectric constant and no ferroelectric instability. In this case the lattice distortion is driven by the polar nature of the surface. Further examples that nanoscale objects can sustain polarity are recently emerging (see [3] and references therein). In the context of tailoring materials properties for device applications, finite size effects in ultrathin oxide films prove to be an exciting area for future research.

[1] W. A. Harrison *et al.*, Phys. Rev. B **18**, 4402 (1978).
[2] N. Nakagawa, H. Y. Hwang, and D. A. Muller, Nature Mater. **5**, 204 (2006).
[3] J. Gonjakowski, F. Finocchi, and C. Noguera, Rep. Prog. Phys. **71**, 016501 (2008).
[4] P. W. Tasker, J. Phys. C **12**, 4977 (1979).
[5] A. Ohtomo and H. Y. Hwang, Nature (London) **427**, 423 (2004).
[6] A. Brinkman *et al.*, Nature Mater. **6**, 493 (2007).
[7] N. Reyren *et al.*, Science **317**, 1196 (2007).
[8] W. Siemons *et al.*, Phys. Rev. Lett. **98**, 196802 (2007).
[9] A. Kalabukhov *et al.*, Phys. Rev. B **75**, 121404(R) (2007).
[10] P. R. Willmott *et al.*, Phys. Rev. Lett. **99**, 155502 (2007).
[11] M. Basletic *et al.*, Nature Mater. **7**, 621 (2008).
[12] M. Sing *et al.*, arXiv:cond-mat/0809.1917.
[13] S. Thiel, G. Hammerl, A. Schmehl, C. W. Schneider, and J. Mannhart, Science **313**, 1942 (2006).
[14] C. Cen *et al.*, Nature Mater. **7**, 298 (2008).
[15] M. Huijben *et al.*, Nature Mater. **5**, 556 (2006).
[16] R. Pentcheva and W. E. Pickett, Phys. Rev. B **74**, 035112 (2006).
[17] S. Gemming and G. Seifert, Acta Mater. **54**, 4299 (2006).
[18] M. S. Park, S. H. Rhim, and A. J. Freeman, Phys. Rev. B **74**, 205416 (2006).
[19] J.-M. Albina *et al.*, Phys. Rev. B **76**, 165103 (2007).
[20] J.-L. Maurice *et al.*, Mater. Sci. Eng. B **144**, 1 (2007).
[21] K. Janicka, J. P. Velev, and E. Tsymbal, J. Appl. Phys. **103**, 07B508 (2008).
[22] Z. Zhong and P. J. Kelly, Europhys. Lett. **84**, 27001 (2008).
[23] R. Pentcheva and W. E. Pickett, Phys. Rev. B **78**, 205106 (2008); Phys. Rev. B **48**, 16929 (1993).
[24] V. I. Anisimov, I. V. Solovyev, M. A. Korotin, M. T. Czyzyk, and G. A. Sawatzky, Phys. Rev. B **48**, 16929 (1993).
[25] P. Blaha *et al.*, WIEN2K, (K. Schwarz, Techn. Univ. Wien, Austria, 2001), ISBN 3-9501031-1-2.
[26] J. P. Perdew, K. Burke, and M. Ernzerhof, Phys. Rev. Lett. **77**, 3865 (1996).
[27] Test calculations within the local density approximation (LDA) using the LDA-lateral lattice parameter of STO (3.85 Å) showed similar structural relaxations within ± 0.02 Å.
[28] V. Vonk *et al.*, Phys. Rev. B **75**, 235417 (2007).
[29] W. Moritz (private communication).
[30] D. R. Hamann, D. A. Muller, and H. Y. Hwang, Phys. Rev. B **73**, 195403 (2006).
[31] S. Okamoto, A. J. Millis, and N. A. Spaldin, Phys. Rev. Lett. **97**, 056802 (2006).
[32] U. Schwingenschlögl and C. Schuster, Europhys. Lett. **81**, 17007 (2008).
[33] We note that nominal charges are frequently used but generally not well defined. Both the use of formal charges (or Born effective charges [17] which may be more appropriate) and the shift by a rigid number of lattice constants is only a rough estimate.
[34] J. Lee and A. A. Demkov, Phys. Rev. B **78**, 193104 (2008).
[35] S. Ishibashi and K. Terakura, J. Phys. Soc. Jpn. **77**, 104706 (2008).
[36] D. D. Fong *et al.*, Science **304**, 1650 (2004).
[37] M. Dawber *et al.*, Phys. Rev. Lett. **95**, 177601 (2005).
[38] L. Despont *et al.*, Phys. Rev. B **73**, 094110 (2006).
[39] For a review or overview, see C. H. Ahn, K. M. Rabe, and J.-M. Triscone, Science **303**, 488 (2004); Ph. Ghosez and J. Junquera, *First-Principles Modeling of Ferroelectric Oxide Nanostructures*, in Handbook of Theoretical and Computational Nanotechnology, edited by M. Rieth and W. Schommers (American Scientific Publishers, Stevenson Ranch, CA, 2006); arXiv:cond-mat/0605299.